encyclopedia

MDPI

Field Guide

Morphometric Characterization of Bacteria Associated with Bacteremia

Ladees Al Hafi [1,2] and Evangelyn C. Alocilja [1,2,*]

[1] Department of Biosystems and Agricultural Engineering, Michigan State University, East Lansing, MI 48824, USA; alhafila@msu.edu
[2] Global Alliance for Rapid Diagnostics (GARD), Michigan State University, East Lansing, MI 48824, USA
* Correspondence: alocilja@msu.edu

Abstract

Among the leading causes of bacteremia are *Escherichia coli*, *Klebsiella pneumoniae*, and *Staphylococcus aureus*. *E. coli* and *K. pneumoniae* are increasingly exhibiting resistance to last-resort antibiotics, such as carbapenems. Rapid and accurate identification of these pathogens is critical for timely treatment and infection control. This paper aimed to develop a computer-aided bacterial morphometric technique for identifying and classifying wild-type *E. coli*, *K. pneumoniae*, and *S. aureus* in a field guide fashion. A 3D laser scanning confocal microscope was used to gather key parameters of each organism: length (L, μm), circular diameter (CD, μm), volume (V, μm^3), surface area-to-cross-sectional area ratio (SA/CSA, unitless), surface uniformity ratio (Str), and surface texture ratio (Sdr). Microscope images and measurement results showed that *S. aureus* was spherical with the shortest length (1.08 μm) and smallest volume (0.52 μm^3). *E. coli* and *K. pneumoniae* were rod-shaped with lengths >2.0 μm and volumes >1.0 μm^3. Carbapenem-resistant (CR) strains exhibited larger volumes than their wild-type counterparts. Surface parameters further differentiated strains: wild-type *E. coli* had a greater surface texture or a less smooth surface (larger Sdr) than *K. pneumoniae* (lower Sdr) did. CR *E. coli* had more surface uniformity (lower Str) than CR *K. pneumoniae* did. A dichotomous key based on shape, circular diameter, volume, length, and surface characteristics was developed to classify the species using a series of paired, contrasting features. This morphometric analysis can aid researchers in quickly identifying bacteria, leading to faster diagnosis of life-threatening diseases and improved treatment decisions.

Keywords: bacteremia; antimicrobial resistance (AMR); diagnostics; dichotomous; morphometrics; size; surface roughness; *E. coli*; *K. pneumoniae*; *S. aureus*

check for updates

Academic Editors: Milva Pepi and Maria Pia Ferraz

Received: 27 May 2025
Revised: 12 August 2025
Accepted: 14 August 2025
Published: 27 August 2025

Citation: Al Hafi, L.; Alocilja, E.C. Morphometric Characterization of Bacteria Associated with Bacteremia. *Encyclopedia* **2025**, *5*, 130. https://doi.org/10.3390/encyclopedia5030130

Copyright: © 2025 by the authors. Licensee MDPI, Basel, Switzerland. This article is an open access article distributed under the terms and conditions of the Creative Commons Attribution (CC BY) license (https://creativecommons.org/licenses/by/4.0/).

1. Introduction

Bacteremia is the presence of viable bacteria in circulating blood, and it is associated with significant morbidity and mortality [1]. Various factors, including microbial infection, medical procedures, or the use of medical devices, can cause bacteremia [1]. In a surveillance study between 2002 and 2020, *Escherichia coli*, *Klebsiella pneumoniae*, and *Staphylococcus aureus* were the top three causes of bacteremia in Taiwan [2]. Sepsis can develop from bacteremia if the body's immune system is unable to control the infection [2]. It can rapidly progress to organ failure and can lead to shock and death if not treated quickly [2]. Rapid and accurate identification of the causative bacteria is crucial for effective treatment. Current methods of identification include culture (colony morphology and biochemical tests),

staining (Gram-positive and Gram-negative stains), genomics (polymerase chain reaction, microarrays, and ribotyping), and other advanced techniques (mass spectrometry and flow cytometry). However, these techniques are time-consuming and expensive. Bacterial identification based on morphology is gaining popularity [3]. It is rapid, reduces costs, and yields intuitive results [3,4]. Modern morphometry utilizes advanced computer-assisted image analysis software to interface an image with geometric software that measures specific biological features [4]. It is a quantitative analysis of the size and shape of geometric features of cells, cell organelles, and/or biomarkers [4]. Bacterial morphometry allows for a systematic approach to bacterial identification, progressing from easily observable characteristics to more detailed microscopic and biochemical analyses. It functions like a field guide by providing a framework for identifying bacteria based on their characteristic shapes, arrangements, and visible growth patterns.

The emergence of bacteria with antimicrobial resistance (AMR) has further exacerbated the poor outcomes associated with bacteremia [2]. The rise in AMR makes diagnosis and treatment increasingly complex [5,6]. AMR is one of the top three major public health threats by the World Health Organization (WHO) and is the third leading cause of death after cardiovascular diseases [6]. An estimated 1.27 million deaths were attributed to antimicrobial-resistant infections in 2019 alone, while nearly 5 million deaths were somehow associated with drug-resistant infections [6]. AMR infections can lead to severe complications, especially among immunocompromised patients [7,8]. Therapeutic options for infections caused by antimicrobial-resistant bacteria are limited, resulting in prolonged illness and significant morbidity and mortality, with a high financial impact [8]. Many medical advances, such as organ transplants and cancer therapy, depend on the ability to fight infections with antimicrobials. If the ability to effectively treat those infections is lost, the ability to safely offer people many of the lifesaving and life-improving modern medical advances will be lost with it.

Beta-lactams, including penicillin, cephalosporin, monobactam, and carbapenem, are the most widely used antibiotics worldwide, and they are reserved only for human use [9]. Carbapenems are the most effective antimicrobial agents against both Gram-positive and Gram-negative bacteria, exhibiting a broad spectrum of antibacterial activity. Thus, the rise in carbapenem-resistant (CR) bacteria is concerning, as it limits treatment options and is associated with increased morbidity, mortality, and healthcare costs [6,10]. CR can induce structural and physiological changes in bacterial cells, potentially altering their morphology and growth patterns [11–13].

Thus, this paper aimed to develop a computer-aided bacterial morphometric technique for identifying and classifying wild-type *Escherichia coli*, *Klebsiella pneumoniae*, and *Staphylococcus aureus* in a field guide fashion [13]. The first classification employed shape, followed by other parameters. Bacteria have distinct shapes, such as (1) spherical or round (cocci), in clusters (e.g., *Staphylococcus*), in chains (e.g., *Streptococcus*), in pairs with pointed ends (e.g., *Streptococcus pneumoniae;*), and in pairs with kidney bean shape (e.g., *Neisseria*); (2) rods (bacilli), with square ends (e.g., *Bacillus*), with rounded ends (e.g., *Salmonella*), club-shaped (e.g., *Corynebacterium*), fusiform (e.g., *Fusobacterium*), and comma-shaped (e.g., *Vibrio*); and (3) spiral (Spirochetes), relaxed coil (e.g., *Borrelia*), and tightly coiled (e.g., *Treponema*) [11].

The morphometric technique was extended to classify CR *E. coli* and CR *K. pneumoniae* since both pathogens are frequently known to develop CR, but not on *S. aureus*, because it is not commonly known to have resistance to carbapenem. By mapping morphometric traits to specific species, this guide supports faster, image-based identification and strengthens the ability to respond to the growing threats of AMR.

2. Materials and Methods

2.1. Instrumentation

A 3D laser scanning confocal microscope (3D-LSCM, Keyence VK-X1000, Itasca, IL, USA, Nano-Biosensors Lab, Michigan State University) was used in this study. In addition to the 3D imaging, several parameters were measured: Feret length (L, μm), Feret width (W, μm), circular diameter (CD, μm), volume (V, μm^3), surface area-to-cross-sectional area ratio (SA/CSA, unitless), surface uniformity ratio (Str), and surface texture ratio (Sdr).

2.2. Source of Isolates

The CR *E. coli* (MDHHS Isolate 17, OXA-48 gene) and CR *K. pneumoniae* (MDHHS Isolate 10, NDM and OXA-48 genes) strains used in this study were selected from the Michigan Department of Health and Human Services (MDHHS) CRE (carbapenem-resistant *Enterobacteriaceae*) reference panel. The wild-type bacteria (*E. coli*, *K. pneumoniae*, and *S. aureus*) were available in the Nano-Biosensors Lab. *E. coli* C3000 is a well-characterized laboratory strain previously described in the literature (ATCC 15597).

2.3. Sample Preparation for 3D Measurements and Imaging

Bacterial cultures of *E. coli*, *K. pneumoniae*, and *S. aureus* were prepared using a glutaraldehyde fixation protocol optimized for morphological preservation. Each species was first grown on its respective selective agar medium (CHROMagar™ *E. coli*, Klebsiella Blue Agar, MacConkey Agar, or CHROMagar™ *S. aureus*, CHROMagar, Saint-Denis, France). Single colonies were used to inoculate Tryptic Soy Broth (TSB) and incubated at 37 °C with shaking overnight. The resulting cultures, adjusted to an optical density equivalent to a McFarland standard of 2 (~6.0×10^8 CFU/mL), were harvested in 1 mL portions and pelleted by centrifugation at 6000× *g* for 3 min. Pellets were rinsed twice with 0.1 M cacodylate buffer (Sigma-Aldrich, St. Louis, MO, USA, UNSPSC Code: 12161706) prior to fixation in 5% glutaraldehyde for 1 h at room temperature. Following fixation, cells were washed twice more in cacodylate buffer (10 min per wash). Fixed samples were mounted onto 1 mm glass slides and stained with Loeffler's methylene blue (Sigma-Aldrich, UNSPSC Code: 12171500) for 10 min to enhance image contrast. For each bacterial species, 250 cells were measured, with samples drawn from two independently prepared cultures on separate days.

This sample size was selected to balance statistical power with practical constraints, such as time, image quality, and computational limitations. Sampling 250 cells per strain ensured adequate representation of intra-strain variability while allowing for meaningful statistical comparisons across groups. This number aligns with sample sizes used in similar morphometric studies and provides a robust dataset for exploratory classification. While larger sample sizes may further enhance resolution, the consistency of trends observed across measurements suggests that the chosen number was sufficient for this study's objectives.

2.4. Resistance Profiling

Antimicrobial susceptibility tests (AST) for carbapenem were performed on *E. coli* and *K. pneumoniae*, but not on *S. aureus*, as it is a Gram-positive bacterium and requires a different class of antibiotics and testing standards.

AST was performed using a modified disk diffusion method (Kirby-Bauer) in accordance with Clinical and Laboratory Standards Institute (CLSI) guidelines [14,15]. Fresh colonies of each bacterial strain were selected from overnight growth on tryptic soy agar (Sigma-Aldrich, UNSPSC Code: 41171605). Colonies were suspended in sterile saline and adjusted to a 0.5 McFarland standard (~1.5×10^8 CFU/mL) using a nephelometer. Mueller-

Hinton agar (Sigma-Aldrich, UNSPSC Code: 41171607) plates were then used for all isolates. A sterile bacterial spreader was used to evenly lawn the bacterial suspension (100 µL) over the surface of the agar in three directions, ensuring uniform coverage. Plates were allowed to dry for 5 min before antibiotic disks were applied. For Gram-negative isolates (*E. coli* and *K. pneumoniae*), three antibiotic disks of Meropenem (Thermo Scientific, Waltham, MA, USA, Catalog: J66446.MF) (10 µg) were used per plate. Inoculated plates were incubated aerobically at 37 °C for 16–18 h. Finally, zone diameters were measured in millimeters using a ruler. Results were interpreted as susceptible (S) for ≥23 mm, intermediate (I) for 20–22 mm, or resistant (R) for ≤19 mm based on CLSI2023 breakpoints [15].

2.5. Sample Measurement

The 3D-LSCM was used to measure morphological parameters in 250 cells per bacterial species. Parameters included Feret horizontal (µm), Feret vertical (µm), circular diameter (CD, µm), volume (V, μm^3), surface area-to-cross-sectional area ratio (SA/CA, unitless), surface uniformity ratio (Str), and surface texture ratio (Sdr). Unlike general Feret diameters, which vary with measurement angle, horizontal and vertical Feret values provide orientation-independent metrics useful for comparing similarly shaped objects of different sizes and for distinguishing elongated from round morphologies. For this study, cell length was defined as the maximum of the two Feret values. Str quantifies surface uniformity, with values approaching 0 indicating smoothness and values near 1 indicating irregularity [16]. Sdr represents the relative increase in surface area contributed by surface texture, ranging from 0 for a flat surface to higher values for sloped or rough surfaces [16]. In addition to these quantitative measures, 3D images of the bacteria were also obtained. Morphometric data for wild-type and CR strains are summarized in Table 1.

Table 1. Average morphometric values of wild-type *Escherichia coli*, *Klebsiella pneumonia*, and *Staphylococcus aureus* and carbapenem-resistant (CR) *Escherichia coli* and *Klebsiella pneumoniae*.

Morphometrics	Wild-Type *Escherichia coli*	Wild-Type *Klebsiella pneumoniae*	Wild-Type *Staphylococcus aureus*	CR *Escherichia coli*	CR *Klebsiella pneumoniae*
Length (L, µm)	2.30 ± 0.12	2.63 ± 0.14	1.08 ± 0.14	2.30 ± 0.22	2.34 ± 0.35
Circle Diameter (CD, µm)	1.73 ± 0.18	1.78 ± 0.19	0.97 ± 0.10	1.82 ± 0.05	1.83 ± 0.06
Volume (V, μm^3)	1.20 ± 0.53	1.40 ± 0.43	0.52 ± 0.23	2.02 ± 0.49	1.87 ± 0.36
Surface Area/Cross-Sectional Area (SA/CA)	1.49 ± 0.12	1.39 ± 0.04	1.47 ± 0.07	1.44 ± 0.06	1.38 ± 0.08
Surface Uniformity (Str)	0.42 ± 0.04	0.35 ± 0.03	0.43 ± 0.05	0.35 ± 0.04	0.40 ± 0.05
Surface Texture (Sdr)	0.56 ± 0.16	0.43 ± 0.06	0.58 ± 0.08	0.47 ± 0.06	0.40 ± 0.09

All values are reported as mean ± standard deviation of 250 measured cells.

2.6. Statistical Analysis

Statistical analysis was performed in Microsoft Excel [11] using one-way ANOVA at a 5% significance level ($\alpha = 0.05$) to assess differences among bacterial sample means. Because classification occurred in a cascading manner, ANOVA was applied at each step. When significant differences were detected ($p < 0.05$), Tukey's Honestly Significant Difference (HSD) post hoc test was used to identify which groups differed.

3. Results

Results from the AST showed that the average zone of inhibition for CR *E. coli* was 21.67 ± 1.70 mm, indicating intermediate resistance, and for *K. pneumoniae*, it was 0 mm, indicating high resistance to meropenem.

Morphological characteristics across bacterial strains were quantified, and average key morphometric features, including cell dimensions, volume, surface area, and surface properties, for wild-type and CR *E. coli* and *K. pneumoniae*, as well as wild-type *S. aureus*, are presented in Table 1.

Graphical and statistical analyses are presented in Figure 1. All comparisons are statistically significant at least at a 5% significance level.

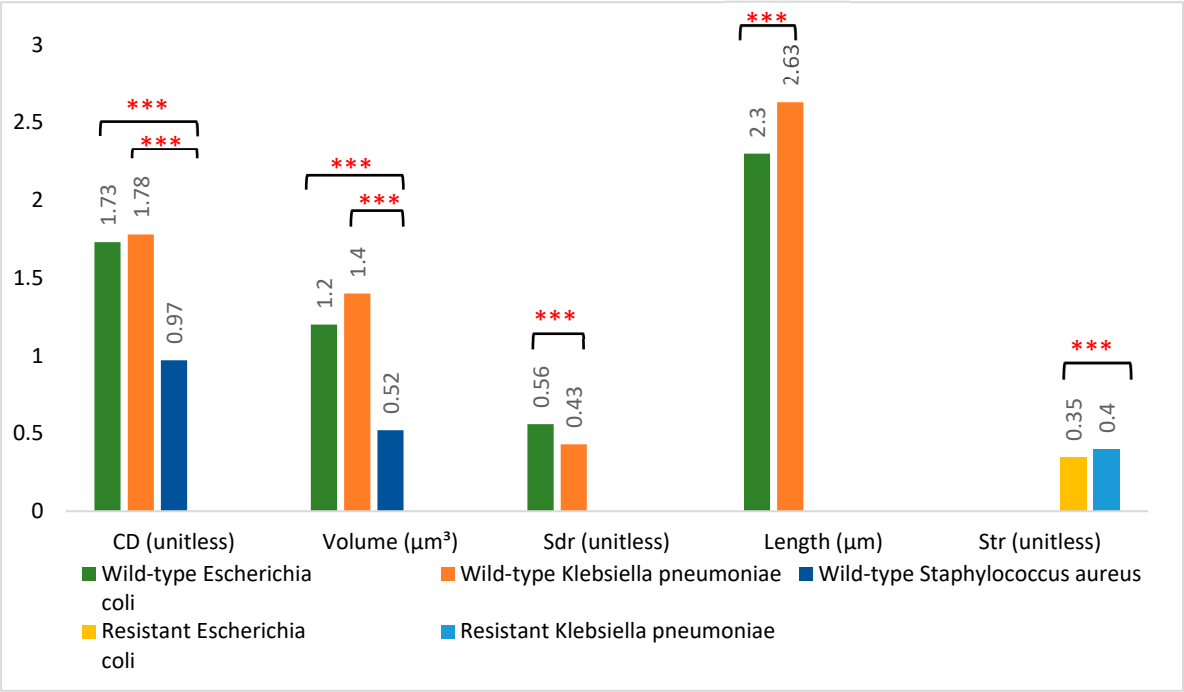


Figure 1. Graphical and statistical analyses of the morphometric measurements of the three bacterial species: *E. coli*, *K. pneumoniae*, and *S. aureus.* All values are statistically significant from each other. The bar graphs represent the mean ± standard deviation of each parameter measured across each of the strains. Statistically significant differences between species for each parameter are indicated by brackets and asterisks (***). *p*-values for interspecies comparisons are as follows: circular diameter (CD): wild-type *E. coli* and *S. aureus* (0), wild-type *K. pneumoniae* and *S. aureus* (0); volume: wild-type *E. coli* and *S. aureus* (1.11×10^{-16}), wild-type *K. pneumoniae* and *S. aureus* (2.22×10^{-16}); Sdr: wild-type *E. coli* and wild-type *K. pneumoniae* (5.55×10^{-16}); length: wild-type *E. coli* and wild-type *K. pneumoniae* (7.87×10^{-6}); Str: CR *E. coli* and CR *K. pneumoniae* (0.00345).

4. Field Guide Dichotomous Classification

Data presented in Table 1 show that wild-type *S. aureus* is spherical, with the shortest length (1.08 ± 0.14 µm) and smallest volume (0.52 ± 0.23 µm^3). Wild-type *E. coli* and *K. pneumoniae* are rod-shaped, with average lengths greater than 2.0 µm, volumes greater than 1.0 µm^3, and circular diameters greater than 1.4 µm. *K. pneumoniae* has less surface texture (smaller Sdr) than *E. coli*. The CR bacteria have larger volumes than the wild-type ones. CR *E. coli* has more surface uniformity (smaller Str value) but has a more textured surface (higher Sdr) than CR *K. pneumoniae*.

Figure 2 presents the dichotomous key for classifying the five organisms as a field guide. Branching decisions are based on distinguishing features such as shape, circular diameter (CD), volume, length, surface texture (Sdr), and uniformity (Str), allowing stepwise

identification of each organism. Threshold values used to separate species are derived from quantitative morphometric analysis. The first step in the dichotomous classification was based on the shape observed from the images of the five bacterial species: either spherical or rod-shaped. Figure 2 shows that *S. aureus* is spherical, while *E. coli* and *K. pneumoniae* are rod-shaped. The second step used the CD, volume, length, Str, and Sdr values to differentiate the rod-shaped bacteria. CR bacteria have an average volume $\geq$1.8 μm^3, distinguishing them from the wild-type bacteria, which have an average volume of <1.8 μm^3. The third step used Str values, where CR *E. coli* has an average Str of <0.4 compared to CR *K. pneumoniae* with an average Str of $\geq$0.4. The final step used Sdr values, where wild-type *E. coli* has an average Sdr $\geq$ 0.5, while wild-type *K. pneumoniae* has an average Sdr < 0.5.

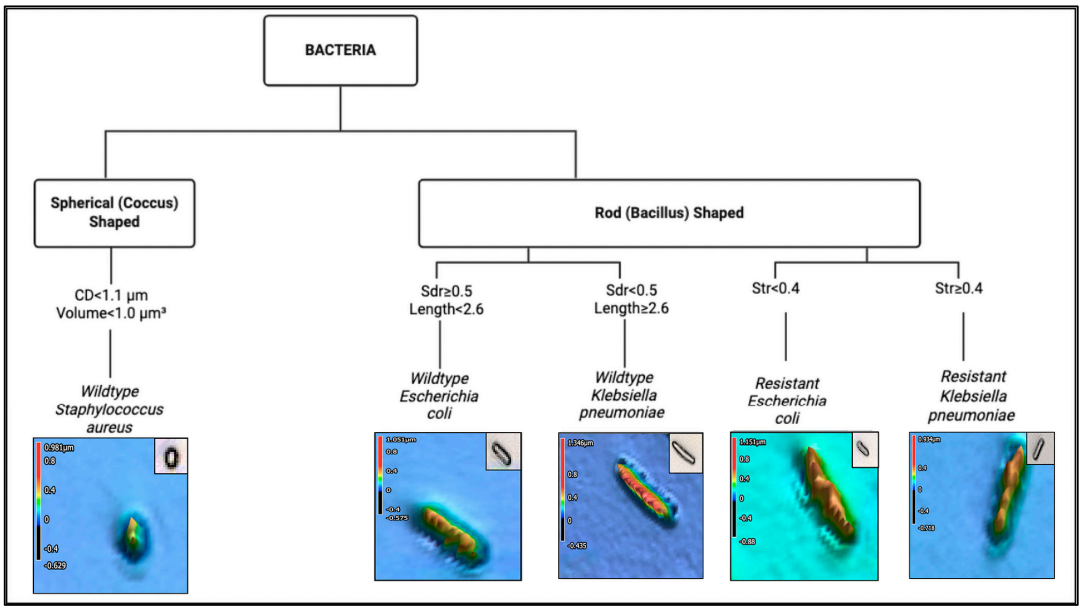


Figure 2. Dichotomous key for differentiating bacterial species based on morphometric and surface parameters.

Figures 3–7 present the 3D images of the bacteria as singular, interacting, and aggregate cells. The images illustrate the surface morphologies, captured using a 3D laser scanning confocal microscope. Wild-type *E. coli* appears as elongated rod-shaped cells. Wild-type *K. pneumoniae* shows a slightly plumper rod shape, with a smoother, less textured surface compared to the wild-type *E. coli*. Wild-type *S. aureus* displays spherical (coccoid) cells, also appearing in clusters. The CR *E. coli* cells exhibit increased surface roughness, as indicated by elevated *Sdr* values. CR *K. pneumoniae* shows less surface uniformity as shown by a higher Str value.

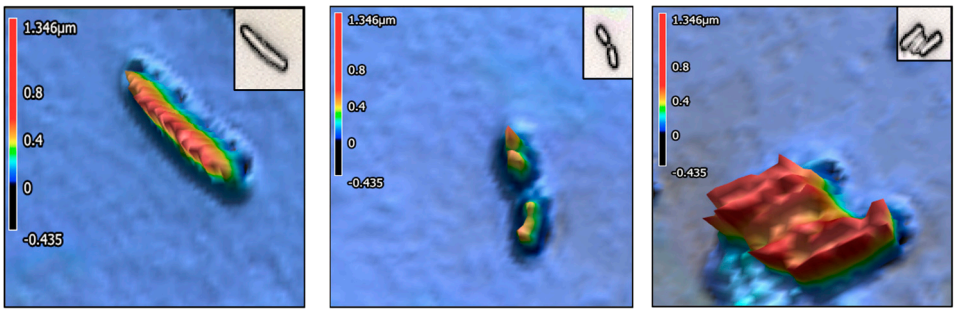
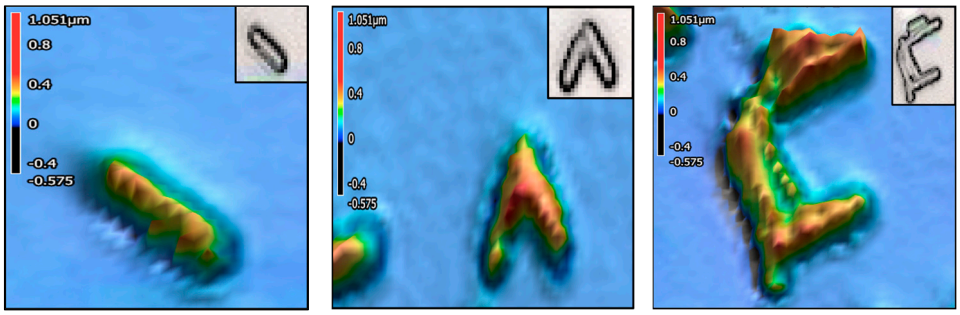
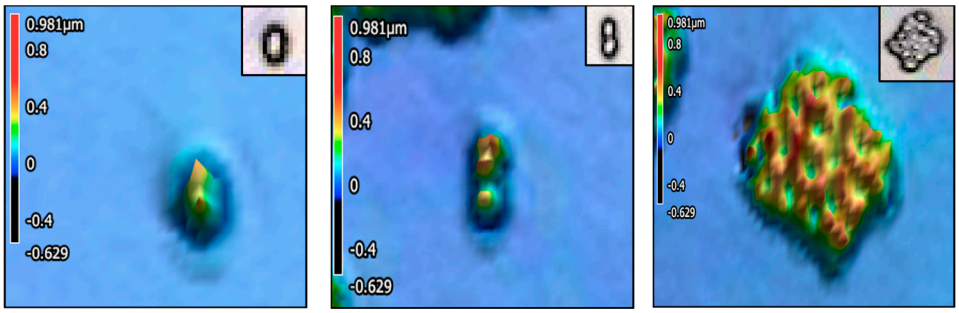


Figure 3. Wild-type *Escherichia coli:* Three-dimensional images with height heatmap of (**a**) singular cell, (**b**) 2 interacting cells, and (**c**) aggregate of more than 3 cells.



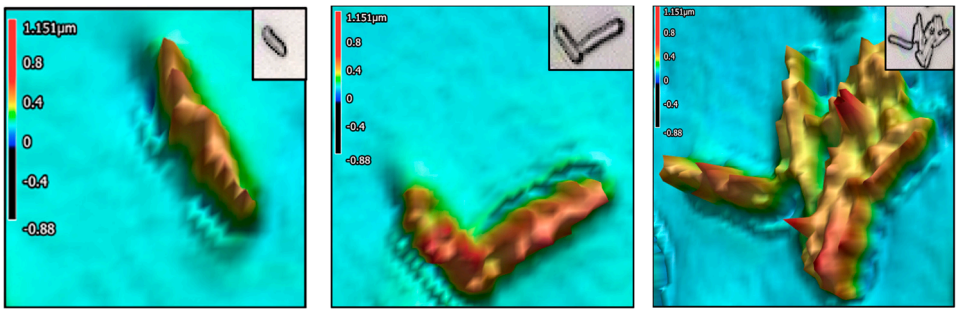
(**a**) (**b**) (**c**)

Figure 4. Wild-type *Klebsiella pneumonia:* Three-dimensional images with height heatmap of (**a**) singular cell, (**b**) 2 interacting cells, and (**c**) aggregate of more than 3 cells.



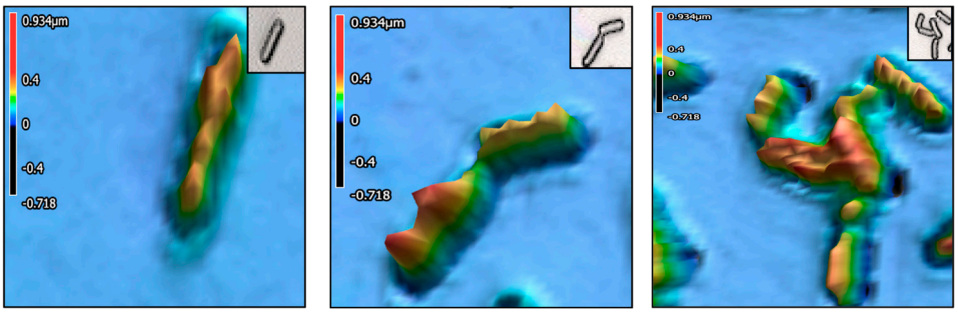
(**a**) (**b**) (**c**)

Figure 5. Wild-type *Staphylococcus aureus*: Three-dimensional images with height heatmap of (**a**) a singular cell, (**b**) 2 interacting cells, and (**c**) an aggregate of more than 3 cells.



(**a**) (**b**) (**c**)

Figure 6. Carbapenem-resistant *Escherichia coli:* Three-dimensional images with height heatmap of (**a**) singular cell, (**b**) 2 interacting cells, and (**c**) aggregate of more than 3 cells.



(**a**) (**b**) (**c**)

Figure 7. Carbapenem-resistant *Klebsiella pneumonia.* Three-dimensional images with height heatmap of (**a**) singular cell, (**b**) 2 interacting cells, and (**c**) aggregate of more than 3 cells.

5. Discussion

5.1. Novelty

Currently, no international standards exist for distinguishing bacterial species based on morphometric features alone; this work is first in its class. The hypothesis was that the identification of morphological differences could become a complement to diagnostic or phenotyping tools. The results represent a preliminary step toward integrating morphometric data into broader classification frameworks.

Results from this study confirm that *S. aureus* has a spherical shape and aggregates into pairs and clusters (Figure 6b,c), supporting the literature. For example, a study shows that *S. aureus* in fixed culture media is 0.5–1.0 µm in diameter and grows in clusters, pairs, and occasionally in short chains [17]. Furthermore, the results show that *E. coli* has a rougher surface (Sdr = 0.56) than *K. pneumoniae* (Sdr = 0.43), which is supported by a previous study showing that *E. coli* colonies can have a range of surface textures, from smooth and flat to bumpy or spread out, while *K. pneumoniae* colonies are more likely to be smooth and dome-shaped [18]. A study shows that *E. coli* colonies are more likely to remain distinct, while *K. pneumoniae* colonies tend to coalesce or merge on the agar plate [18]. Results from this study demonstrate similar behaviors as shown in Figure 3b,c for *E. coli* with distinct cells and Figure 4b,c for *K. pneumoniae* with merging cells.

Carbapenem-resistant Enterobacteriaceae, such as *K. pneumoniae* and *E. coli*, have gained resistance to carbapenem drugs by acquiring carbapenemase genes [9]. These results show that the volumes of wild-type *E. coli* and *K. pneumoniae* (1.20 μm^3 and 1.40 μm^3, respectively) are smaller than those of the resistant strains (2.02 μm^3 and 1.87 μm^3, respectively). These results agree with findings where antibiotic-resistant strains showed differences in morphology from the sensitive parental strain, and the differences were most prominent in the β-lactam-resistant bacteria [9]. A cluster analysis revealed increased proportions of fatter cells (higher volume) in the antibiotic-resistant strains [13]. A correlation analysis of morphological features and gene expression suggested that genes related to energy metabolism and antibiotic resistance were highly correlated with the morphological characteristics of the resistant strains [13].

5.2. Strengths

A key strength of this study lies in its standardized and reproducible protocol for preparing and imaging bacterial samples using morphometric analysis. By applying consistent fixation and staining methods across multiple species, comparability was established between samples, which is essential for maintaining reliable morphometric baselines. The inclusion of both wild-type and CR strains from several clinically relevant species strengthens the generalizability of the findings and highlights the method's potential for broader applications in rapid species identification and antimicrobial resistance (AMR) profiling. Additionally, the quantitative nature of the data collected provides a rich dataset that can inform the development of phenotypic screening tools or machine learning classifiers.

5.3. Limitations

This study has obvious limitations. First, while over 250 cells were analyzed per species, data were derived from only two biological replicates per strain, which may not fully capture within-strain variability. Bacterial morphology measurements are difficult to replicate due to a combination of factors, including environmental influences, inherent cellular variability, and the complexity of shape regulation mechanisms. Even within the same species, cells can exhibit significant variations in size and shape, and these variations can be further affected by changes in growth conditions. So, while bacterial morphology is a genetically determined trait, it is also a dynamic and adaptable characteristic that is influ-

enced by a complex interplay of environmental and cellular factors, making it challenging to achieve perfect replication of morphology measurements across different experiments and even within the same experiment over time. Second, although a range of bacterial species was included, this study did not assess intra-species diversity across multiple clinical isolates, which would be necessary for real-world diagnostic applications. Third, while morphometric changes were observed between resistant and wild-type strains, the study did not directly validate these findings with molecular or functional resistance assays, limiting the ability to conclude causality between phenome and genome characteristics. Finally, as the analysis was conducted under controlled laboratory conditions, further validation in clinical or environmental settings is needed to confirm the robustness and utility of the approach. Despite these limitations, this study offers a practical and scalable framework for morphometric characterization that can inform future efforts to develop rapid, affordable bacterial classification and AMR screening tools.

6. Conclusions

The objective of this study was to rapidly classify wild-type bacterial strains and compare CR properties within the same species using detailed morphometric analysis. By quantifying cellular parameters, it is observed that wild-type strains of *E. coli*, *Klebsiella pneumoniae*, and *S. aureus* can be differentiated with statistically significant results. Additionally, significant differences in surface texture (Str) values ($p < 0.05$) were found between CR *E. coli* and *K. pneumoniae*. These results indicate that morphometric profiling can serve as a rapid and informative tool for the early identification of wild-type bacteria, and those more likely to respond to antibiotics. This approach holds promise in the fight against bacteremia, sepsis, and antimicrobial resistance, offering a potential preliminary screening method to identify resistant phenotypes and guide treatment decisions before time-consuming AST and molecular confirmatory tests are conducted.

Author Contributions: Conceptualization, L.A.H. and E.C.A.; methodology, L.A.H.; software, L.A.H.; validation, L.A.H.; formal analysis, L.A.H. and E.C.A.; data curation, L.A.H.; writing—original draft preparation, L.A.H.; writing—review and editing, L.A.H. and E.C.A.; supervision, E.C.A.; project administration, E.C.A.; funding acquisition, E.C.A. In addition, L.A.H. performed all measurements using the Keyence 3D Laser Confocal Scanning VK-X1000 Microscope (Keyence Corporation, Osaka, Japan). All authors have read and agreed to the published version of the manuscript.

Funding: Research related to this article was supported by the USDA Hatch MICL 02782, USDA Hatch Multistate NC1194 MICL 04233 (RA101064), and USDA-NIFA project 2022-67017-36982.

Data Availability Statement: The data presented in this study are available on request from the corresponding author, due to file size limitations.

Acknowledgments: The authors thank the Michigan Department of Health and Human Services (MDHHS) for providing the carbapenem-resistant (CR) isolates used in the study.

Conflicts of Interest: The authors declare no conflicts of interest.

References

1. McNamara, J.F.; Righi, E.; Wright, H.; Hartel, G.F.; Harris, P.N.A.; Paterson, D.L. Long-term morbidity and mortality following bloodstream infection: A systematic literature review. *J. Infect.* **2018**, *77*, 1–8. [CrossRef] [PubMed]
2. Huang, Y.-C.; Kuo, S.-C.; Fang, C.-T.; Lauderdale, T.-L. Changing epidemiology and antimicrobial resistance of bacteria causing bacteremia in Taiwan: 2002–2020. *Microbiol. Spectr.* **2024**, *12*, e00608–e00624. [CrossRef] [PubMed]
3. Al Hafi, L.; Franco, A.J.; Kao, K.; Alocilja, E.C. Field Guide: Morphometric Visualization and Characterization of Selected Foodborne Pathogens Using Advanced Imaging Techniques. *Encyclopedia* **2025**, *5*, 47. [CrossRef]
4. Wang, X.; Shi, Y.; Guo, S.; Qu, X.; Xie, F.; Duan, Z.; Hu, Y.; Fu, H.; Shi, X.; Quan, T.; et al. A Clinical Bacterial Dataset for Deep Learning in Microbiological Rapid On-Site Evaluation. *Sci. Data* **2024**, *11*, 608. [CrossRef] [PubMed]

5. Abban, M.K.; Ayerakwa, E.A.; Mosi, L.; Isawumi, A. The burden of hospital acquired infections and antimicrobial resistance. *Heliyon* **2023**, *9*, e20561. [CrossRef] [PubMed]
6. Salam, M.A.; Salam, A.; Al-Amin, Y.; Pawar, J.S.; Akhter, N.; Rabaan, A.A.; Alqumber, M.A.A. Antimicrobial Resistance: A Growing Serious Threat for Global Public Health. *Healthcare* **2023**, *11*, 1946. [CrossRef] [PubMed]
7. Abbara, S.; Guillemot, D.; Smith, D.R.; El Oualydy, S.; Kos, M.; Poret, C.; Breant, S.; Brun-Buisson, C.; Watier, L. Antimicrobial Resistance as Risk Factor for Recurrent Bacteremia after *Staphylococcus aureus*, *Escherichia coli*, or *Klebsiella* spp. Community-Onset Bacteremia. *Emerg. Infect. Dis.* **2024**, *30*, 974–983. [CrossRef] [PubMed]
8. Elbehiry, A.; Marzouk, E.; Aldubaib, M.; Moussa, I.; Abalkhail, A.; Ibrahem, M.; Hamada, M.; Sindi, W.; Alzaben, F.; Almuzaini, A.M.; et al. Pseudomonas species prevalence, protein analysis, and antibiotic resistance: An evolving public health challenge. *AMB Express* **2022**, *12*, 53. [CrossRef] [PubMed]
9. Meletis, G. Carbapenem resistance: Overview of the problem and future perspectives. *Ther. Adv. Infect. Dis.* **2016**, *3*, 15–21. [CrossRef] [PubMed]
10. Ahmed, S.K.; Hussein, S.; Qurbani, K.; Ibrahim, R.H.; Fareeq, A.; Mahmood, K.A.; Mohamed, M.G. Antimicrobial resistance: Impacts, challenges, and future prospects. *J. Med. Surg. Public Health* **2024**, *2*, 100081. [CrossRef]
11. Levinson, W.; Chin-Hong, P.; Joyce, E.A.; Nussbaum, J.; Schwartz, B. Structure of Bacterial Cells. In *Review of Medical Microbiology & Immunology: A Guide to Clinical Infectious Diseases*, 16th ed.; McGraw Hill: New York, NY, USA, 2020. Available online: https://accessmedicine.mhmedical.com/content.aspx?bookid=3123&sectionid=261995947 (accessed on 30 June 2025).
12. Amako, K.; Meno, Y.; Takade, A. Fine structures of the capsules of Klebsiella pneumoniae and Escherichia coli K1. *J. Bacteriol.* **1988**, *170*, 4960–4962. [CrossRef] [PubMed]
13. Ikebe, M.; Aoki, K.; Hayashi-Nishino, M.; Furusawa, C.; Nishino, K. Bioinformatic analysis reveals the association between bacterial morphology and antibiotic resistance using light microscopy with deep learning. *Front. Microbiol.* **2024**, *15*, 1450804. [CrossRef] [PubMed]
14. Hudzicki, J. Kirby-Bauer disk diffusion susceptibility test protocol. *Am. Soc. Microbiol.* **2009**, *15*, 1–23.
15. Clinical and Laboratory Standards Institute. *Breakpoint Implementation Toolkit*; Clinical and Laboratory Standards Institute: Malvern, PA, USA, 2024. Available online: https://clsi.org/resources/breakpoint-implementation-toolkit/ (accessed on 15 June 2025).
16. Corporation, K. Sal (Auto-Correlation Length) | Area Roughness Parameters. Keyence America. Available online: https://www.keyence.com/ss/products/microscope/roughness/surface/sal-auto-correlation-length.jsp (accessed on 30 June 2025).
17. Foster, T. Staphylococcus. In *Medical Microbiology*, 4th ed.; Baron, S., Ed.; University of Texas Medical Branch at Galveston: Galveston, TX, USA, 1996. Available online: http://www.ncbi.nlm.nih.gov/books/NBK8448/ (accessed on 20 May 2025).
18. Klebsiella Pneumoniae and *Escherichia coli* on Endo Agar Plate. Metallic Sheen Around *E. coli* Colonies. Available online: https://www.microbiologyinpictures.com/bacteria-photos/klebsiella-pneumoniae-photos/klebsiella-ecoli-endo-agar.html (accessed on 21 May 2025).

Disclaimer/Publisher's Note: The statements, opinions and data contained in all publications are solely those of the individual author(s) and contributor(s) and not of MDPI and/or the editor(s). MDPI and/or the editor(s) disclaim responsibility for any injury to people or property resulting from any ideas, methods, instructions or products referred to in the content.